Experimental study of the effect of a small bubble at the nose of a larger bubble in a Hele-Shaw cell

E. Ikeda and T. Maxworthy*
Department of Aerospace Engineering, University of Southern California, Los Angeles, California 90089-1191
(Received 29 June 1989)

The effect of a small air bubble attached to the nose of a much larger air bubble in a viscous liquid in a Hele-Shaw cell has been studied. The Hele-Shaw cell was tilted to an angle α, measured from the horizontal, so that the buoyancy force allowed the bubbles to rise. The larger bubble became elongated to a nearly elliptical shape and its velocity increased above the value for a circular bubble of the same area. For a given size of main bubble, as the size of the nose bubble decreased, the aspect ratio and velocity of the larger bubble increased. The velocity for a given size bubble could be approximated by the theory presented by Maxworthy [J. Fluid Mech. **173**, 95 (1986)] for small values of the bubble ellipticity and large values of α. At small values of α, modification of the bubble drag by gravitational distortion could partially explain the deviation from the simpler theory.

I. INTRODUCTION

During the study of the motion of an isolated bubble in a Hele-Shaw cell,[1] an interesting phenomenon was observed. When a small bubble became accidently attached to the nose of a much larger bubble, the larger bubble became elongated and its velocity increased manyfold (Ref. 1, Fig. 4). It was hypothesized that this was due to the small bubble causing a change in slope and curvature at the nose of the larger bubble, which in turn affected its entire shape, a conjecture recently put in mathematical terms by Hong[2] and Hong and Family.[3] Here this effect has been studied in more detail by varying the size of both the nose and large bubble in a consistent fashion, thus changing the velocity of the bubbles. These elongated bubbles are dynamically similar to the long, narrow fingers first observed by Couder *et al.*[4]

II. EXPERIMENTAL SETUP

A Hele-Shaw cell was constructed from two $30\times90\times1.91$ cm^3 flat Lucite sheets bolted together and separated by a 0.180-cm-thick, 1-cm-wide metal strip. The cell was not quite filled with silicone oil with a kinematic viscosity of 1.06 cm^2/s, as measured using a Cannon-Fenske routine-type viscometer at the operating temperature of the cell. Air was injected at the center of the lower end of the cell to form the large bubble and the cell was then tilted and the bubble allowed to rise under the influence of the buoyancy force on the bubble. The tilt of the cell and the bubble volume were varied in order to change the velocity and shape of the bubbles. A small hole, 8.9 cm from the point where the main air supply was injected, was drilled in the top Lucite sheet in order to introduce the smaller nose bubble. A syringe was used to inject this air into the oil. The large bubble then rose to meet and attach to the smaller bubble.

An RCA, solid-state, color video camera was used to record the motion of the bubbles onto video tape. A clock in the camera, which was also recorded to tape, was used to determine the velocity of the bubbles by timing their motion between marks on the top plate a known distance apart.

For a given tilt of the Hele-Shaw cell from the horizontal α, the length and width of both nose and large bubbles were measured and their velocity was determined. A single parameter was used to characterize the size (area) of the large and nose bubbles; R and r, respectively, are the square root of the product of the length (L) and width (D) of the elliptical bubbles, i.e., the diameter of the equivalent circular bubble. The range of R was from 1 to 10 cm, and the range of r was from 0.3 to 0.8 cm. The values of α used were 7.43°, 10.24°, 13.26°, 17.88°, and 20.70°.

III. RESULTS AND DISCUSSION

When the nose bubble was too small, it was pushed aside by the larger bubble, and did not attach to it. If the nose bubble was too large, the bubbles joined, but interaction between them caused the nose bubble to oscillate, which in turn caused oscillations of the larger bubble [Ref. 1, Fig. 4(d)]. There was only a certain range of size of nose bubbles which resulted in the production of stable, elongated bubbles. Under all circumstances these bubbles had a nearly elliptical shape (Fig. 1).

As shown in Ref. 1, Fig. 4(a), the elongated bubble was due to the small bubble changing the boundary conditions of the larger bubble at the location where the two were in contact. The larger bubble changed its slope and radius of curvature at these points to match that of the smaller bubble. With this increased curvature at its tip, the larger bubble became more slender and its velocity increased. With a fixed α, it was found that for a given R, the smaller the nose bubble (decreasing r), the larger the aspect ratio of the larger bubble (L/D) became (Fig. 2), because the smaller nose bubble caused the larger bubble to become even more curved at its tip. However, for $r\equiv0$, i.e., the case where there was no nose bubble, the

larger bubble was not elongated,[1] the aspect ratio was approximately 1, and thus this represents a singular case. An understanding of how the shape of the bubble was affected as r approached zero could not be made since, as already noted, small bubbles, of order of the gap width or less, would not attach to the larger ones.

From the results for all values of α the R versus L/D graph (Fig. 3), there is a clear dependence of the bubble's aspect ratio on α, with the bubble being more elongated at the higher values of α. This was expected since a larger buoyancy force would cause the bubble to rise more quickly, making it more streamlined. Cross-plotting the data as r/R versus L/D (Fig. 4), the nose bubble effect on the aspect ratio seems to depend only weakly on α, with only the two smaller values contributing almost all of the variance.

As given by Ref. 1, the bubble velocity can be approximated by

$$U \approx \frac{h^2 g' \sin\alpha}{12\nu_1} \left[\frac{L}{D}\right] \left[\frac{D}{L}\right]_{U'=2}$$

where $g'=g[(\rho_1-\rho_2)/\rho_1]$, g is the gravitational constant, ρ is the fluid density, h is the cell thickness,

$$\left[\frac{D}{L}\right]_{U'=2} = \pi\lambda \frac{1}{\tanh^{-1}[\sin(\pi\lambda)]},$$

$\lambda=D/W$, W represents the width of cell, and the subscripts 1 and 2 represent the silicone oil and air, respectively. $(D/L)_{U'=2}$ is a factor used previously to account for the effect of a finite cell width on the bubble shape and velocity, where U' is the ficticious velocity introduced by Taylor and Saffman.[5]

For a fixed α, the velocity for bubbles, when normal-

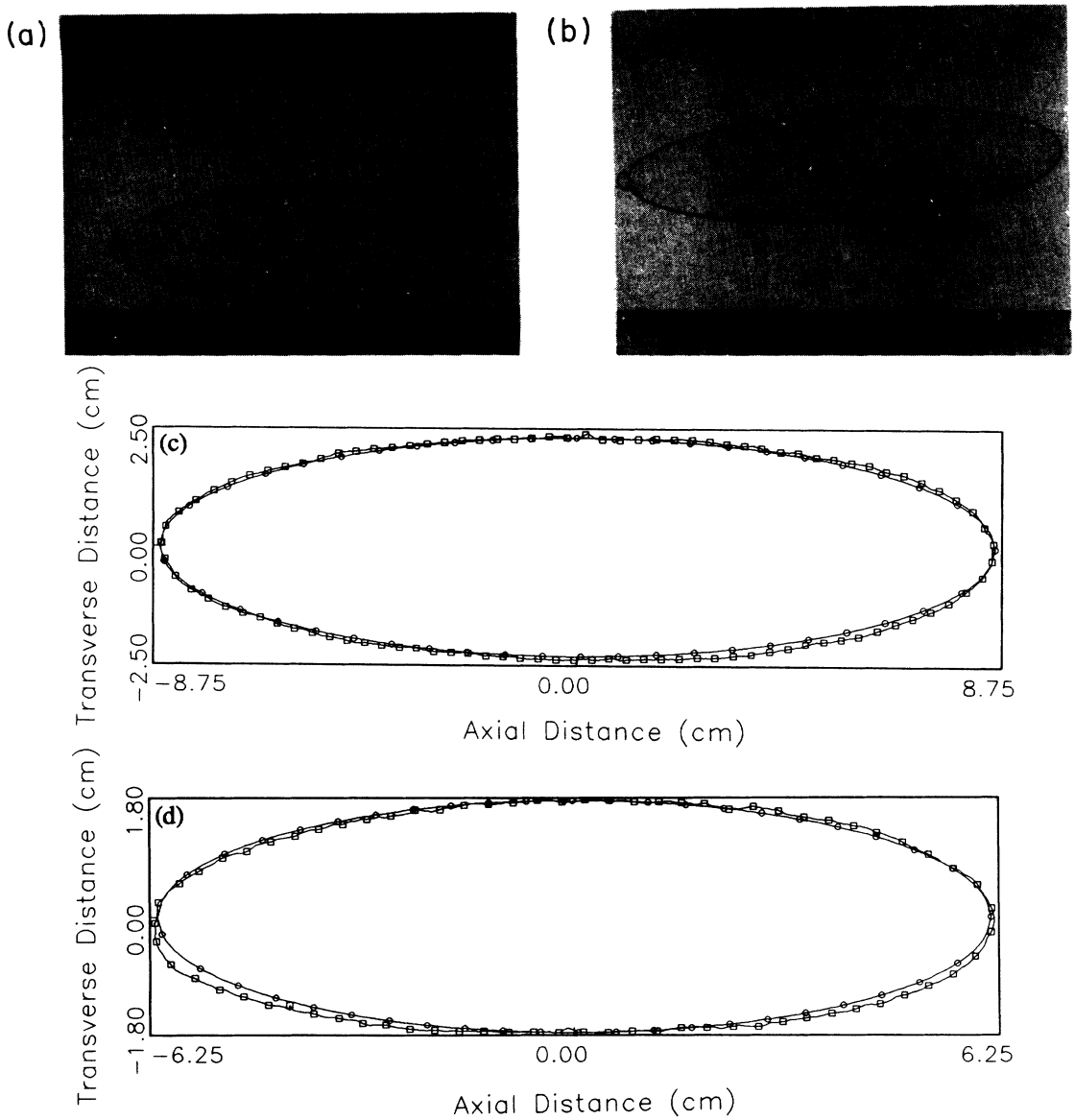

FIG. 1. Bubble is moving to the left. (a) Photograph of bubble with tip bubble ($\alpha=7.43°$). $L/D=3.08$, $R=8.86$ cm, and $r=0.83$ cm. (b) Photograph of bubble with tip bubble ($\alpha=7.43°$). $L/D=3.91$, $R=8.98$ cm, and $r=0.62$ cm. (c) Comparison of bubble shape with ellipse of the same L/D ratio $\alpha=7.43°$. □, bubble shape; ○, ellipse of the same L/D. (d) Comparison of bubble shape with ellipse of the same L/D ratio $\alpha=20.70°$. □, bubble shape; ○, ellipse of the same L/D.

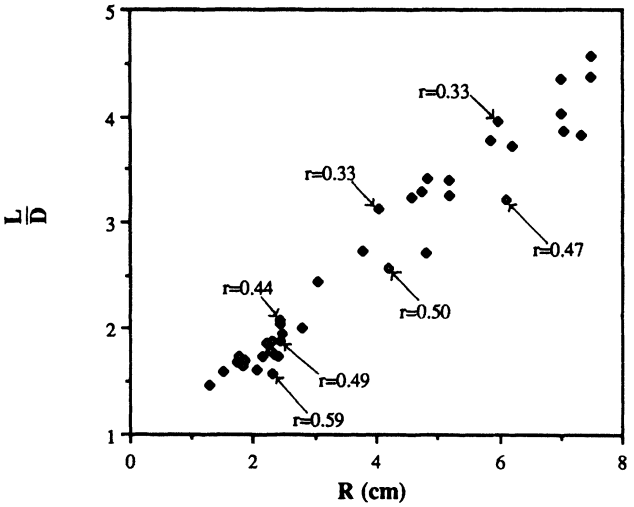

FIG. 2. $-L/D$ versus bubble size R showing that the smaller the nose bubble (r in cm), the larger the aspect ratio for a given value of R ($\alpha = 17.88°$).

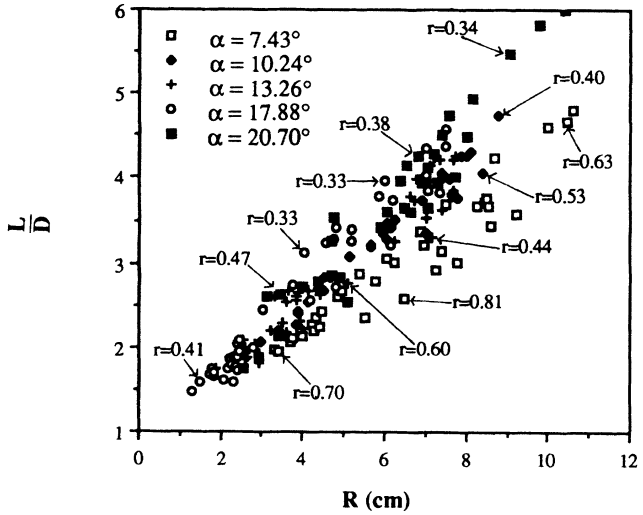

FIG. 3. Raw data of bubble shape vs R with α as parameter with some representative nose bubble sizes r in cm.

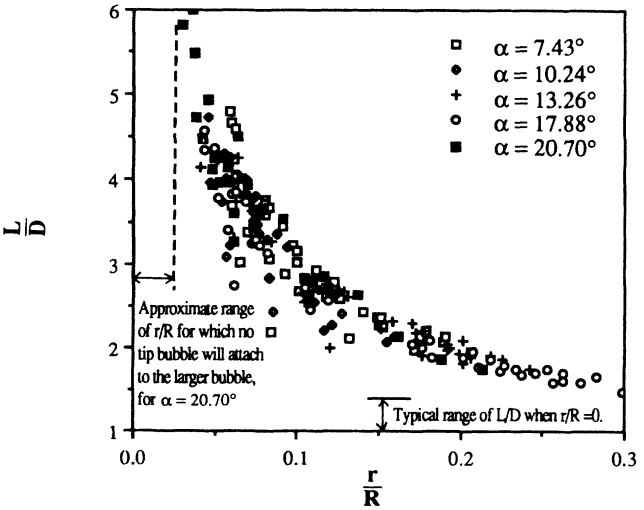

FIG. 4. L/D as a function of r/R for all values of α tested.

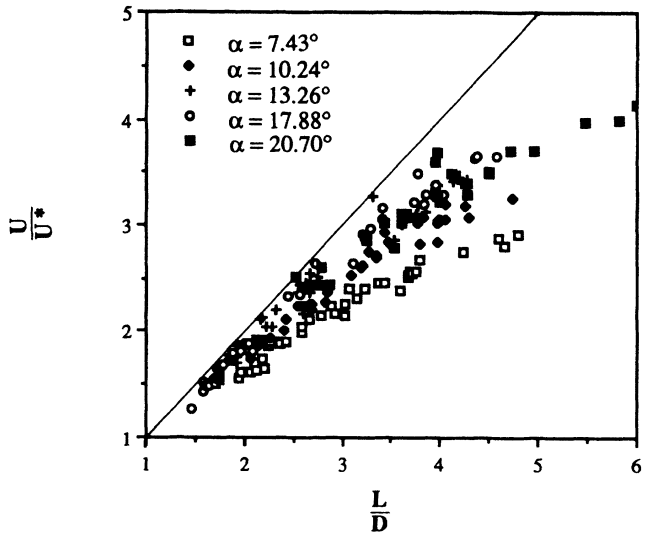

FIG. 5. Normalized bubble velocity vs bubble shape. Theoretical result from Ref. 1 superimposed.

ized with

$$U^* = \frac{h^2 g' \sin\alpha}{12\nu_1} \left[\frac{D}{L}\right]_{U'=2},$$

followed the trend of the above theory for small L/D, though it was consistently smaller for the smaller values of α (Fig. 5). For increasing L/D, the velocities appear to be approaching asymptotic values. These asymptotes deviate further from the theory for smaller α. The reasons for this deviation from the theory are far from clear. As in one hypothesis, one might assume that at the smaller values of α, and hence smaller absolute values of U, gravitational distortion of the bubble cross section might account for an increase in the dissipation at the perimeter and hence, in the drag experienced by the bubble. This could possibly be measured by a factor such as $g'h^2/\nu U$ (which could be as large as 100 in the present

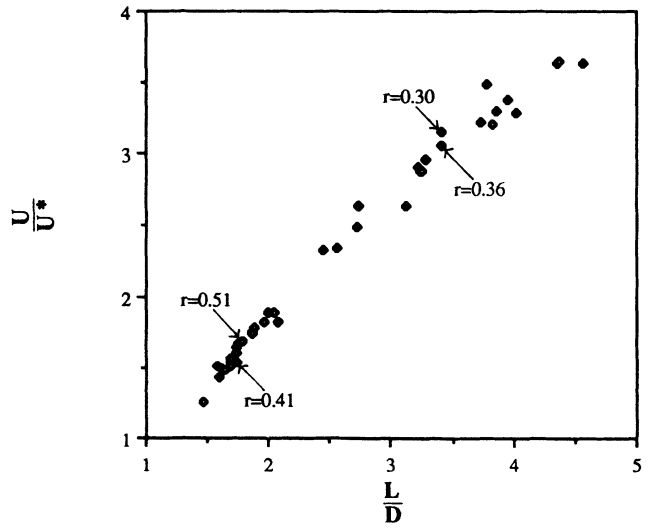

FIG. 6. U/U^* vs L/D showing that the scatter does not seem to depend on the nose bubble size r in cm ($\alpha = 17.88°$).

experiments; see Ref. 1) modified by some geometric factor which accounts for the increased perimeter-area ratio as L/D increased. Attempts to reduce the data of Fig. 5 in this way were only moderately successful and still resulted in an effect of α, for small α, which, however, was somewhat smaller than the variations shown in Fig. 5. Also, for a fixed L/D, it might be expected that the velocity would be higher for larger tip bubbles because there would be the extra buoyancy affect of the nose bubble (Fig. 6). This effect of r on the velocity was not evident and thus, can be concluded that the additional buoyancy effect from the nose bubble was not significant.

IV. CONCLUSIONS

The shape of the a bubble in a Hele-Shaw cell is extremely sensitive to the boundary condition at its nose. When a small bubble becomes attached to a large bubble in a Hele-Shaw cell, it changes the slope and curvature at the tip of the latter so that the large bubble becomes elongated into a shape which is closely elliptical. This hypothesis first introduced in Ref. 1 has recently been given a mathematical interpretation by Hong[2] and Hong and Family[3] who introduced a new independent parameter $\Delta\theta$, the angle of the intersecting surfaces at the tip. Unfortunately, there seems to be no way to determine this angle *a priori* since it depends, in the real case, on the details of the viscous flow around the small bubble in the presence of large surface tension effects. Such a study is beyond the scope of the present study since it requires a numerical calculation of considerable complexity. Because the bubble's aspect ratio increases, its velocity also increases. The velocity of these elongated bubbles can be approximated by

$$U \approx \frac{h^2 g' \sin\alpha}{12\nu_1} \left[\frac{L}{D}\right] \left[\frac{D}{L}\right]_{U'=2}$$

for small L/D. At larger aspect ratios and smaller values of R, the increased drag possibly due to gravitational distortion of the bubble becomes significant. Further tests, possibly in a cell with a smaller gap, are required to obtain a fuller understanding of the effect of the nose bubble as r/R approaches zero, the case of no nose bubble.

---

*Also at Department of Mechanical Engineering, University of Southern California, Los Angeles, CA 90089-1453.

[1]T. Maxworthy, J. Fluid Mech. **173**, 95 (1986).

[2]D. C. Hong, Phys. Rev. A **39**, 2042 (1989).

[3]D. C. Hong, and F. Family, Bull. Am. Phys. Soc. **34**, 2330 (1989).

[4]Y. Couder, O. Cardoso, D. Dupuy, P. Tavernier, and W. Thom, Europhys. Lett. **2**, 437 (1986).

[5]G. I. Taylor, and P. G. Saffman, Q. J. Mech. Appl. Math. **12**, 265 (1959).

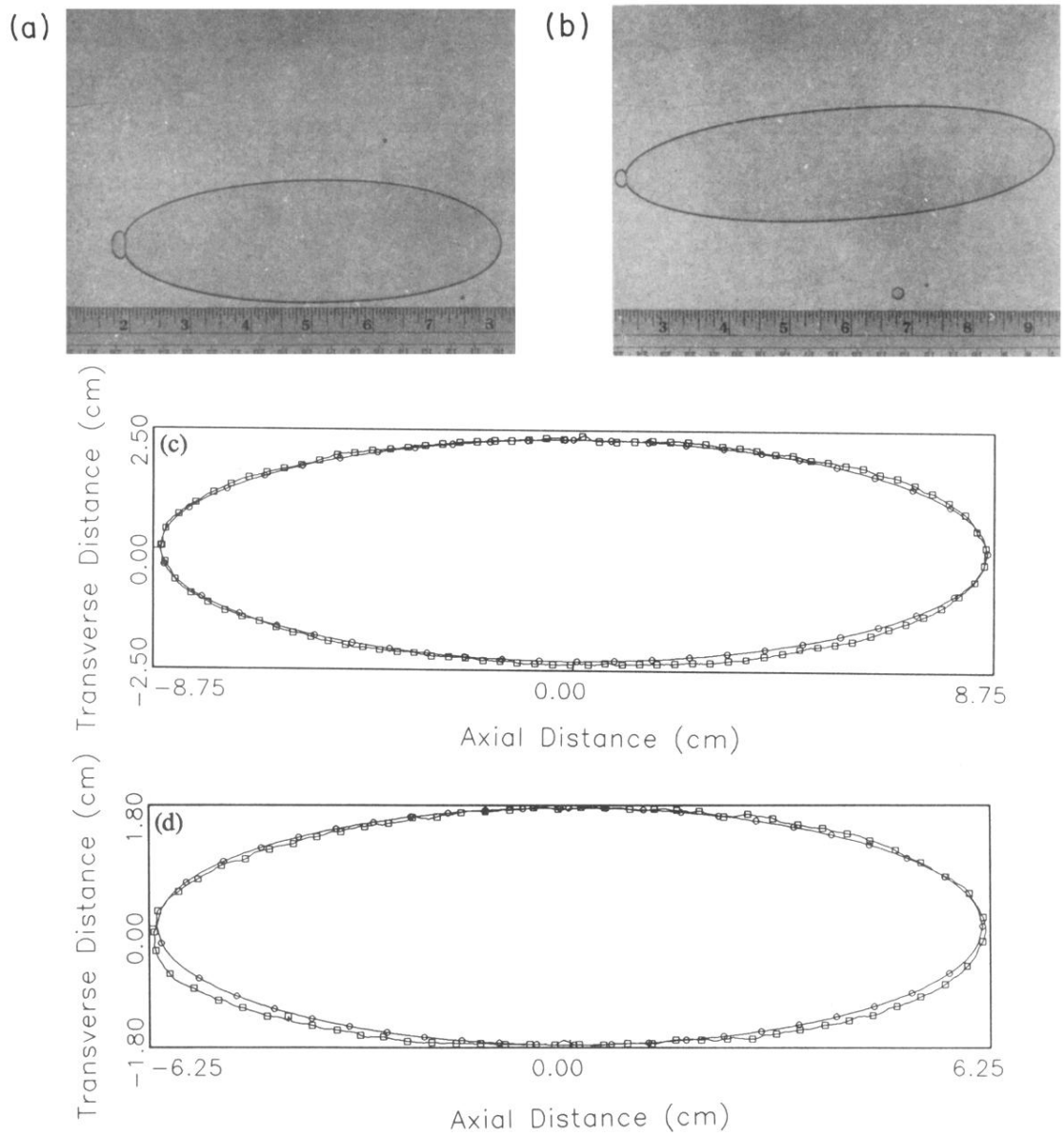

FIG. 1. Bubble is moving to the left. (a) Photograph of bubble with tip bubble ($\alpha = 7.43°$). $L/D = 3.08$, $R = 8.86$ cm, and $r = 0.83$ cm. (b) Photograph of bubble with tip bubble ($\alpha = 7.43°$). $L/D = 3.91$, $R = 8.98$ cm, and $r = 0.62$ cm. (c) Comparison of bubble shape with ellipse of the same L/D ratio $\alpha = 7.43°$. □, bubble shape; ○, ellipse of the same L/D. (d) Comparison of bubble shape with ellipse of the same L/D ratio $\alpha = 20.70°$. □, bubble shape; ○, ellipse of the same L/D.